2004 International Symposium on Nonlinear
Theory and its Applications (NOLTA2004)
Fukuoka, Japan, Nov. 29 - Dec. 3, 2004

Experimental Analysis of Flexibly Coupled Two Rotors

Yohta KUNITOH†, Hiroshi YABUNO††, Hossain Md. Zahid‡, Tsuyoshi INOUE‡, and Yukio ISHIDA‡

†Graduate School of Systems and Information Engineering, University of Tsukuba
1-1-1 Tennodai, Tsukuba-shi, Ibaraki 305-8573, Japan,
††Institute of Engineering Mechanics and Systems, University of Tsukuba
1-1-1 Tennodai, Tsukuba-shi, Ibaraki 305-8573, Japan,
Email: kunitoh@aosuna.esys.tsukuba.ac.jp, yabuno@esys.tsukuba.ac.jp
‡Department of Electronic-Mechanical Engineering, School of Engineering, Nagoya University
Furo-cho, Chikusa-ku, Nagoya 464-8603 , Japan,
Email: ishida@nuem.nagoya-u.ac.jp

Abstract—Rotating machineries are the most widely used elements in mechanical systems. In many systems, such as power plant and jet engine, the rotating machinery is multi-span rotor, which is supported by multiple bearings. In this research, we consider a 2-DOF nonlinear rotary system in which the two nonlinear rotors are coupled by means of a weakly linear stiffness. We show nonlinear normal modes in this system using the method of multiple scales. Furthermore, we indicate the occurrence of mode localization in this system.

1. Introduction

Rotating machineries, such as steam turbines, gas turbines and motors, are the most widely used elements in mechanical systems. However, the rotating parts of such machineries often become the main source of vibration. Hence, analyzing the source of vibration is the critical issue, in order to enhance the stability and the reliability of mechanical systems. In many systems, such as power plant and jet engine, the rotating machinery is multi-span rotor, which is supported by multiple bearings. Therefore, the multi-span rotor is characterized as the system in which each rotor with nonlinear spring characteristic is coupled by means of a weakly linear stiffness. In these systems, there is a possibility of the occurrence of mode localization[1]˜[3] as indicated in the multiple degree of freedom spring-mass systems. Recently, also in the nonlinear systems such as multi-span rotor, nonlinear normal modes has attracted attention [4]˜[6].

In this research, we consider a 2-DOF nonlinear rotary system in which the two nonlinear rotors are coupled by means of a weakly linear stiffness. We show nonlinear normal modes in this system using the method of multiple scales. Then, we indicate the occurrence of mode localization in this system. Furthermore, we experimentally observe the orbits of rotors.

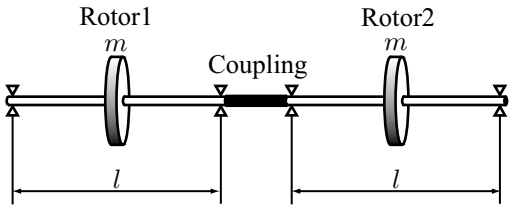

Figure 1: Analytical model

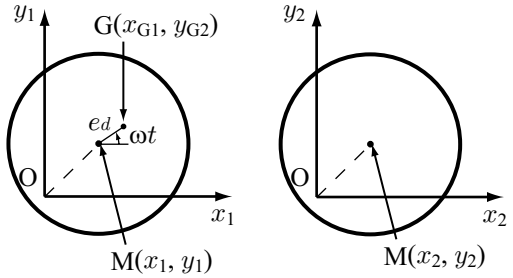

(a) Rotor1 (b) Rotor2

Figure 2: Coordinate system

2. Analytical model and dimensionless equation of motion

As shown in Fig. 1, we consider the behavior of the system in which the two Jeffcott rotors are coupled by means of a weakly linear stiffness. Here, Jeffcott rotor is the rotor in which a rigid disk is mounted at the center of a massless elastic shaft supported at both ends by ball bearings. We introduce the coordinate system as shown in Fig. 2. The origin O of the coordinate system O-xy coincides with the bearing centerline. In Fig. 2, the point G of rotor 1 deviates slightly (e_d) from the geometrical center M, where G and M are the center of gravity and the geometrical center, respectively. On the other hand, the setup of rotor 2 is well-assembled. Moreover, considering the cubic nonlinearity from the characteristic of spring of bearing and the shaft elongation, the equation of motion of the system can

be written as follows:

$$m\ddot{x}_1 + c_d\dot{x}_1 + kx_1 + \gamma_d x_2 + \beta_d(x_1^2 + y_1^2)x_1 = me_d\omega^2\cos\omega t \quad (1)$$
$$m\ddot{y}_1 + c_d\dot{y}_1 + ky_1 + \gamma_d y_2 + \beta_d(x_1^2 + y_1^2)y_1 = me_d\omega^2\sin\omega t \quad (2)$$
$$m\ddot{x}_2 + c_d\dot{x}_2 + kx_2 + \gamma_d x_1 + \beta_d(x_2^2 + y_2^2)x_2 = 0 \quad (3)$$
$$m\ddot{y}_2 + c_d\dot{y}_2 + ky_2 + \gamma_d y_1 + \beta_d(x_2^2 + y_2^2)y_2 = 0, \quad (4)$$

where ω, c_d, k, β_d and γ_d are the angular velocity, the viscous damping coefficient, the linear spring constant of the elastic shaft, the nonlinear spring constant and the linear spring constant of the coupling, respectively.

Next, we rewrite Eqs. (1)-(4) in the dimensionless form. Using the inverse value of the frequency $\Omega = \sqrt{k/m}$ as the representative time T_r and the span l as the representative length, we set the dimensionless parameters as follows:

$$t = (1/\Omega)t^*,\ \ x_1 = lx_1^*,\ \ y_1 = ly_1^*,\ \ x_2 = lx_2^*,\ \ y_2 = ly_2^*.$$

Hereafter the asterisk is omitted.

Hence, we obtain the following dimensionless equations:

$$\ddot{x}_1 + c\dot{x}_1 + x_1 + \gamma x_2 + \beta(x_1^2 + y_1^2)x_1 = e\nu^2\cos\nu t \quad (5)$$
$$\ddot{y}_1 + c\dot{y}_1 + y_1 + \gamma y_2 + \beta(x_1^2 + y_1^2)y_1 = e\nu^2\sin\nu t \quad (6)$$
$$\ddot{x}_2 + c\dot{x}_2 + x_2 + \gamma x_1 + \beta(x_2^2 + y_2^2)x_2 = 0 \quad (7)$$
$$\ddot{y}_2 + c\dot{y}_2 + y_2 + \gamma y_1 + \beta(x_2^2 + y_2^2)y_2 = 0, \quad (8)$$

where the dimensionless parameters, e^*, c^*, γ^*, β^* and ν^*, are expressed as follows:

$$e^* = \frac{e_d}{l},\ \ c^* = \frac{c_d}{\sqrt{mk}},\ \ \gamma^* = \frac{\gamma_d}{k},\ \ \beta^* = \frac{\beta_d l^2}{k},\ \ \nu^* = \frac{\omega}{\Omega}.$$

3. Derivation of the approximate solution using the method of multiple scales

We analyze Eqs. (5)-(8) as 4-DOF equations of oscillations. By using a small parameter ϵ ($|\ \epsilon\ | \ll 1$) as a booking device, we quantitatively set the magnitudes of the parameters as follows:

$$e = \epsilon^3\hat{e},\quad c = \epsilon^2\hat{c},\quad \gamma = \epsilon^2\hat{\gamma},$$

where ($\hat{}$) denotes "of the order $O(1)$". We seek the approximate solutions of Eqs. (5)-(8) in the form

$$x_1 = \epsilon x_{11} + \epsilon^3 x_{13} + \cdots \quad (9)$$
$$y_1 = \epsilon y_{11} + \epsilon^3 y_{13} + \cdots \quad (10)$$
$$x_2 = \epsilon x_{21} + \epsilon^3 x_{23} + \cdots \quad (11)$$
$$y_2 = \epsilon y_{21} + \epsilon^3 y_{23} + \cdots. \quad (12)$$

We introduce the multiple time scales as follows:

$$t_0 = t,\ t_2 = \epsilon^2 t,$$

where t_0 is the fast time scale, and t_1 is slow time scale. By applying the method of multiple scales, the following approximate solutions are obtained:

$$x_1 = a_{x1}\cos(\nu t + \varphi_{x1}) + O(\epsilon^3) \quad (13)$$
$$y_1 = a_{y1}\cos(\nu t + \varphi_{y1}) + O(\epsilon^3) \quad (14)$$
$$x_2 = a_{x2}\cos(\nu t + \varphi_{x2}) + O(\epsilon^3) \quad (15)$$
$$y_2 = a_{y2}\cos(\nu t + \varphi_{y2}) + O(\epsilon^3). \quad (16)$$

Then, a_{x1}, φ_{x1}, a_{y1}, φ_{y1}, a_{x2}, φ_{x2}, a_{y2} and φ_{y2} are computed by solving the following set of eight modulation equations:

$$\frac{d}{dt}a_{x1} = -\frac{1}{2}ca_{x1} + \frac{1}{2}\gamma a_{x2}\sin(\varphi_{x1} - \varphi_{x2}) + \frac{1}{8}\beta a_{x1}a_{y1}^2\sin 2(\varphi_{x1} - \varphi_{y1}) - \frac{1}{2}e\sin\varphi_{x1} \quad (17)$$
$$a_{x1}\frac{d}{dt}\varphi_{x1} = -\sigma a_{x1} + \frac{1}{2}\gamma a_{x2}\cos(\varphi_{x1} - \varphi_{x2}) + \frac{3}{8}\beta a_{x1}^3 + \frac{1}{4}\beta a_{x1}a_{y1}^2 + \frac{1}{8}\beta a_{x1}a_{y1}^2\cos 2(\varphi_{x1} - \varphi_{y1}) - \frac{1}{2}e\cos\varphi_{x1} \quad (18)$$
$$\frac{d}{dt}a_{y1} = -\frac{1}{2}ca_{y1} + \frac{1}{2}\gamma a_{y2}\sin(\varphi_{y1} - \varphi_{y2}) - \frac{1}{8}\beta a_{x1}^2a_{y1}\sin 2(\varphi_{x1} - \varphi_{y1}) - \frac{1}{2}e\cos\varphi_{y1} \quad (19)$$
$$a_{y1}\frac{d}{dt}\varphi_{y1} = -\sigma a_{y1} + \frac{1}{2}\gamma a_{y2}\cos(\varphi_{y1} - \varphi_{y2}) + \frac{3}{8}\beta a_{y1}^3 + \frac{1}{4}\beta a_{x1}^2a_{y1} + \frac{1}{8}\beta a_{x1}^2a_{y1}\cos 2(\varphi_{x1} - \varphi_{y1}) + \frac{1}{2}e\sin\varphi_{y1} \quad (20)$$
$$\frac{d}{dt}a_{x2} = -\frac{1}{2}ca_{x2} - \frac{1}{2}\gamma a_{x1}\sin(\varphi_{x1} - \varphi_{x2}) + \frac{1}{8}\beta a_{x2}a_{y2}^2\sin 2(\varphi_{x2} - \varphi_{y2}) \quad (21)$$
$$a_{x2}\frac{d}{dt}\varphi_{x2} = -\sigma a_{x2} + \frac{1}{2}\gamma a_{x1}\cos(\varphi_{x1} - \varphi_{x2}) + \frac{3}{8}\beta a_{x2}^3 + \frac{1}{4}\beta a_{x2}a_{y2}^2 + \frac{1}{8}\beta a_{x2}a_{y2}^2\cos 2(\varphi_{x2} - \varphi_{y2}) \quad (22)$$
$$\frac{d}{dt}a_{y2} = -\frac{1}{2}ca_{y2} - \frac{1}{2}\gamma a_{y1}\sin(\varphi_{y1} - \varphi_{y2}) - \frac{1}{8}\beta a_{x2}^2a_{y2}\sin 2(\varphi_{x2} - \varphi_{y2}) \quad (23)$$
$$a_{y2}\frac{d}{dt}\varphi_{y2} = -\sigma a_{y2} + \frac{1}{2}\gamma a_{y1}\cos(\varphi_{y1} - \varphi_{y2}) + \frac{3}{8}\beta a_{y2}^3 + \frac{1}{4}\beta a_{x2}^2a_{y2} + \frac{1}{8}\beta a_{x2}^2a_{y2}\cos 2(\varphi_{x2} - \varphi_{y2}), \quad (24)$$

where $\nu = 1 + \sigma$.

4. Mode localization

In Fig. 3, the frequency response curves are depicted when $c = 2.14 \times 10^{-3}$, $\gamma = -1.09 \times 10^{-2}$, $\beta = 2.52 \times$

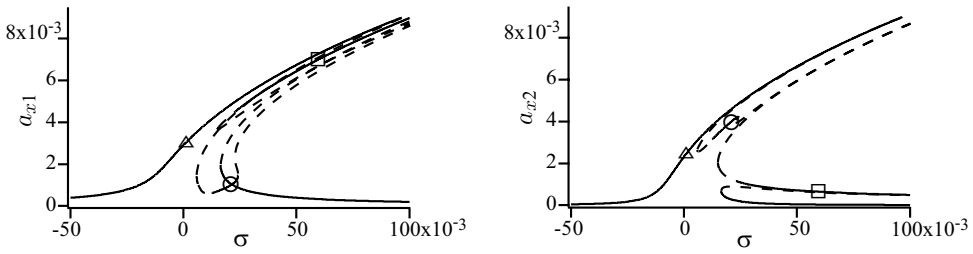

(a) x direction of rotor1 (b) x direction of rotor2

Figure 3: Frequency response curve ($c = 2.14 \times 10^{-3}$, $\gamma = -1.09 \times 10^{-2}$, $\beta = 2.52 \times 10^{3}$, $e = 3.85 \times 10^{-5}$, —— : stable, - - - - : unstable)

10^3 and $e = 3.85 \times 10^{-5}$, these values correspond to those of the subsequent experiment. The solid and dashed lines denote stable and unstable equilibrium points, respectively. From Eqs. (5)-(8), the motions in the x and y-directions are symmetric, the vibrations in the x-direction has the same amplitude as in the y-direction, and the phase difference of $\pi/2$ from in the y-direction. It can be found that bifurcated nonlinear normal modes are localized. Mode localization occurs as shown with the symbols ◯ and □ in Fig. 3.

Figures 4-6 express the orbits of rotors at the rotor speeds shown with the symbols △, ◯ and □ in Fig. 3. At the condition of the symbol △, where the nonlinear normal modes is not bifurcated, the amplitude of rotor 1 is almost equal to that of rotor 2 as shown in Fig. 4. At the symbol ◯, even though the rotor 1 has unbalance, the amplitude of rotor 2 is much larger than that of rotor 1 as shown in Fig. 5. Due to the occurrence of such a response, there is a possibility of wrong diagnosis that rotor 2 has unbalance. On the other hand, this phenomenon indicates that the rotor 2 can be utilized as a dynamic vibration absorber. At the symbol □, the amplitude of rotor 1 is much larger than that of rotor 2 as shown in Fig. 6. The usage of this phenomenon prevents the influence of the oscillation in the rotor 1 caused by the unbalance on the rotor 2.

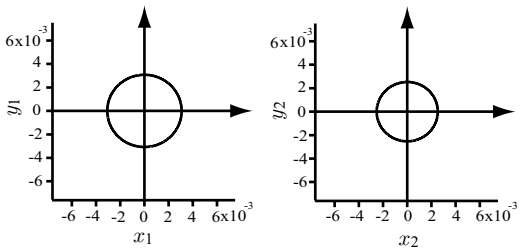

(a) Rotor1 (b) Rotor2

Figure 4: Theoretical orbit ($\sigma = 0.0015$, at the symbol △ in Fig. 3)

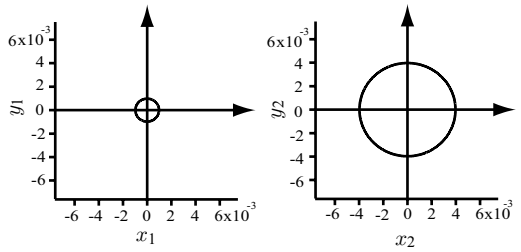

(a) Rotor1 (b) Rotor2

Figure 5: Theoretical orbit ($\sigma = 0.0207$, at the symbol ◯ in Fig. 3)

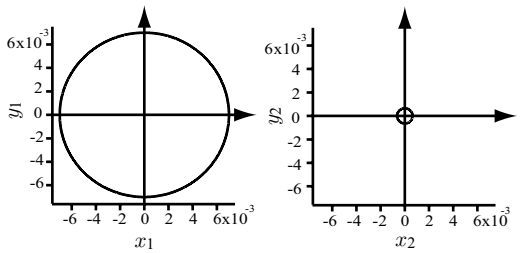

(a) Rotor1 (b) Rotor2

Figure 6: Theoretical orbit ($\sigma = 0.0597$, at the symbol □ in Fig. 3)

5. Experiments

5.1. Experimental setup

Figure 7 shows the experimental setup. An elastic shaft with circular cross section with a length $l = 0.708$ m and a diameter 1.2×10^{-2} m is supported at both ends by a self-aligning double-ball bearing (♯1200) and a single-row deep groove ball bearing (♯6804). A disk is mounted at the center of the shaft. The disk is 0.3 m in diameter and 8.21 kg. The two rotors like this are coupled by spring in imitation of a flange type shaft coupling. The shaft is driven by the three-phase induction motor (Meidensha Corp., TIS85–NR) through V-belt and V-pulley. The motions of disks and the angular velocities are measured from the laser sensors and the rotary encoders, respectively. Other parameters are as follows:

$k = 3.28 \times 10^4$ N/m, $\beta_d = 1.65 \times 10^8$ N/m^3, $\gamma_d = -358$ N.

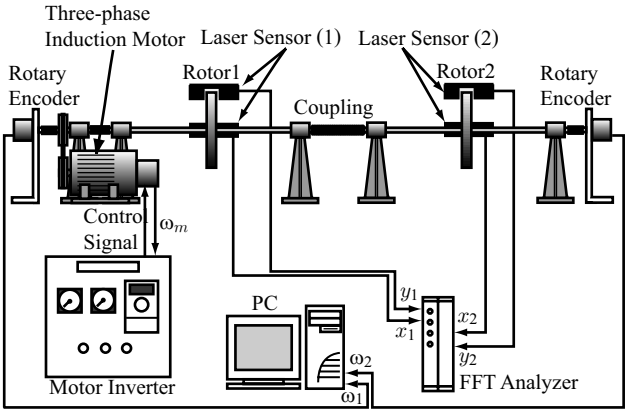

Figure 7: Experimental setup

5.2. Experimental results and discussion

In Figs. 8-10, we show the experimantal orbits of the rotors. In previous section, we analyzed the motion of rotor as circular motion. Indeed, the experimental motion can be expressed the elliptical motion as a summation of forward whirling motion and backward whirling motion. Therefore, we compare the amplitudes of orbits afterward. In the case ω_r(angular velocity)$\times 60/2\pi$ = 600 rpm, the amplitude of rotor 1 is almost equal to that of rotor 2 as shown in Fig. 8. Moreover, in the case $\omega_r \times 60/2\pi$ = 641 rpm, even though rotor 1 has unbalance, the amplitude of rotor 2 is larger than that of rotor 1 as shown in Fig. 9. On the other hand, in the case $\omega_r \times 60/2\pi$ = 624 rpm, the amplitude of rotor 1 is much larger than that of rotor 2 as shown in Fig. 10. We experimentally confirm the occurrence of theoretically predicted two types of mode localizations.

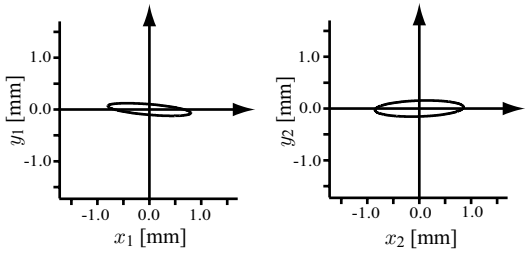

(a) Rotor1 (b) Rotor2

Figure 8: Experimental orbit ($\omega_r \times 60/2\pi$ = 600 rpm)

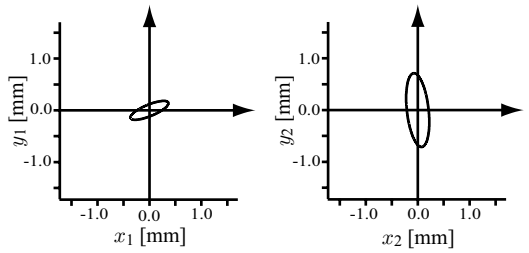

(a) Rotor1 (b) Rotor2

Figure 9: Experimental orbit ($\omega_r \times 60/2\pi$ = 641 rpm)

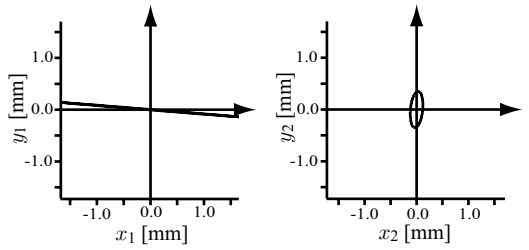

(a) Rotor1 (b) Rotor2

Figure 10: Experimental orbit ($\omega_r \times 60/2\pi$ = 624 rpm)

6. Conclusions

In this research, we investigate the nonlinear normal modes in 2-DOF nonlinear rotary system in which the two nonlinear rotors are coupled by a weakly linear stiffness. Analyzing the equations of motion as 4-DOF equations of oscillations, we show the occurrence of mode localizations in this system. Moreover, based on mode localization, we indicate the possibility of vibration suppression and wrong diagnosis. Furthermore, we experimentally observe theoretically predicted mode localizations.

Acknowledgments

This work was supported by TEPCO Research Foundation.

References

[1] Vakakis, A. F., Manevitch, L. I., Mikhlin, Y. V., Pilipchuk, V. N., and Zevin, A. A., Normal Modes and Localization in Nonlinear Systems, (1996), John Wiley & Sons, Inc., New York.

[2] Aubrecht, J. and Vakakis, A. F., Localized and Non-Localized Nonlinear Normal Modes in a Multi-Span Beam With Geometric Nonlinearities, Journal of Vibration and Acoustics, **118** (1996), 553–542.

[3] Pierre, C., Tang, D. M. and Dowell, E. H., Localized Vibrations of Disordered Multispan Beams: Theory and Experiment, AIAA Journal, **25**-9 (1987), 1249–1257.

[4] Pesheck, E., Pierre, C. and Shaw, S. W., Accurate Reduced-Order Models for a Simple Rotor Blade Model Using Nonlinear Normal Modes, Mathematical and Computer Modeling, **33** (2001), 1085–1097.

[5] Yabuno, H. and Nayfeh A. H., Nonlinear Normal Modes of a Parametrically Excited Cantilever Beam, Nonlinear Dynamics, **25** (2001), 65–77.

[6] Kanda, R., Yabuno, H., Zahid, H. Md., Inoue, T., and Ishida, Y., Nonlinear Normal Modes in 2-DOF Nonlinear System under Forced Excitation, D&D Conference 2003 CD-ROM, No. 419 (2003) (in Japanese).

[7] Yamamoto, T., and Ishida, Y., Linear and Nonlinear Rotordynamics, (2001), John Wiley & Sons, Inc., New York.